https://doi.org/10.48047/AFJBS.6.12.2024.5570-5576

African Journal of Biological Sciences

Journal homepage: http://www.afjbs.com

Research Paper Open Access

Effect of Annealing Temperature on Fractal Characteristic of $Bi_2Fe_4O_9$Nanoparticles

Vivek Kumar Bajpai[1], Ajeet Kumar Rai[1],R.R. Awasthi[2*], K.C. Dubey[3]

[1]Department VIAET, Mechanical Engineering, Shuats, Prayagraj-211007

[2]Faculty of engineering and technology, KhwajaMoinuddin Chishti Language University Lucknow, 226013, U.P., India

[3]Department of Physics, Shia P. G. College, Lucknow-226003, U.P., India

Email:bajpai.vivek4@gmail.com

Article History
Volume 6, Issue 12, 2024
Received: 30 June 2024
Accepted: 20 July 2024
Doi:
10.48047/AFJBS.6.12.2024.5570-5576

Abstract

The main objective of this study was to investigate the effects of annealing temperatures ranging from 500 °C to 550 °C on spray pyrolysis technique $Bi_2Fe_4O_9$ thin films. The presence of no intermediate impurity phases in the $Bi_2Fe_4O_9$ sample was confirmed by X-ray diffraction (XRD), which indicates that the phase is typical orthorhombic with Pbnm space group. According to Scherer's equation, the average crystallite sizes were determined to be 23 nm. Atomic force microscopy (AFM) demonstrated that $Bi_2Fe_4O_9$ NPs are symmetrically dispersed nanorods with a topographic shape on the films' surface.An increase in annealing temperature causes the surface roughness to increase from around 6.76 nm to 8.67 nm, indicating a modification in the thin film's crystal structure. After observation, the fractal dimension values were determined to be 1.78 and 2.06. It is evident that the fractal dimension increases as the annealing temperature rises, from 500 °C to 550 °C, respectively. This finding suggests that can be used to characterize how the whole grain shape varies along the growth direction. Furthermore, the fractal dimension has spatial and profile deviation information, in contrast to RMS roughness.

Keywords: Multiferroics; fractal dimension; $Bi_2Fe_4O_9$; XRD;AFM

1.Introduction

Since potentially couple ferroelectric and antiferromagnetic orders in the same phase, multiferroic materials have garnered a lot of attention in recent decades [1, 2]. As a result, the discovery of the magnetoelectric (ME) effect has been viewed as potentially beneficial for the creation of novel functional devices. At room temperature, single phase multiferroic materials with low energy consumption are extremely rare [3]. For the purpose of improving the ferroelectric and magnetic characteristics, single phase nano-structured powder fabrication is necessary. The multiferroic bismuth ferrite is a well-liked bismuth-based material with good ferroelectric order that is frequently utilized in high temperature magnetoelectric coupling devices.Multiferroic materials can be prepared using a variety of sophisticated processes that can modify the surface area to volume ratio and enhance their microstructural and magnetic characteristics.It is also reported the

substantial magnetoelectric coupling near room temperature in $Bi_2Fe_4O_9$for ME device application [4] method, solid state reaction, and other well-known instances of similar procedures are examples of these. The $Bi_2Fe_4O_9$ oxide was synthesized by a sol-gel approach using polyvinyl alcohol (PVA) as a complex agent calcined at 700 °C from Mn+/–OH = 2:1 precursor shows weak ferromagnetism [5].Densely packed single-crystal $Bi_2Fe_4O_9$ nanowires were successfully synthesized by a template-induced citrate-based sol–gel process and explain the possible formation mechanism of nanowire [6]. The sheet-like $Bi_2Fe_4O_9$ nanoparticles were successfully synthesized by a rather facile hydrothermal process [7].

Commercial use of $Bi_2Fe_4O_9$and $BiFeO_3$ is hampered by its inherent problems, which include high leakage, high loss, poor polarization, changing oxidation state (+2, +3, +4) of Fe, and associated phases. Replacement of Fe ions by 3dtransition ions such as Cr, Mn, Co, Ni, and Cu is also expected to enhance magnetic moments and magnetic anisotropies, improving the magnetic, optical, and ferroelectric characteristics of nanostructure thin films [8–13].However, metal oxide nanostructures have found widespread use in current technology, despite their restricted fractal analysis in functional devices [14]. In this study, we looked at how the annealing temperature affected the spray pyrolysis prepared $Bi_2Fe_4O_9$thin films.

2. Experimental

High purity chemicals used were bismuth nitrate $Bi(NO_3)_3.5H_2O$ (≥99 %, Merck) and iron nitrate $Fe(NO_3)_3.9H_2O$(≥99 %, Merck). These materials were weighedaccurately in suitable stoichiometric amounts. Iron nitrate andbismuth nitrate were dissolved in1:2 molar ratios. To obtain a homogeneous, transparent precursor solution, the mixture was constantly agitated for two hours at room temperature. Methanol and acetone, two organic solvents, were also used to clean the glass substrates in order to get rid of any dust or other contaminants that might have gotten onto the surface. The precursor solutions were sprayed onto the glass substrates at 400 °C for five minutes while maintaining a 0.2 ml/min solution flow rate, assisted by a nebulizer. To achieve the proper crystallization, the as-synthesised thin films were annealed for three hours at 500 °C to 550 °C in an open-air setting using a SiC furnace. Atomic Force Microscope Nanomagnetic Instruments and Rigaku Ultima IV (CuKα ~ 1.5404 Å) were used in X-ray diffraction (XRD) to evaluate the structural and morphological features of pure nanomaterials.

3. Results and discussion

3.1. Structural analysis

The XRD pattern of BFO nanostructures is shown in Figure 1(a). The XRD peaks that were found have a good match with the orthorhombiccrystal structureJCPDS (80-8638) with the Pbam space group. The $Bi_2Fe_4O_9$ XRD pattern does not show any intermediate impurity phases. Scherer's equation was used to calculate the average crystallite sizes of $Bi_2Fe_4O_9$ thin films that were annealed between 500 °C to 550 °C.

$D = \frac{K\lambda}{\beta \cos\theta}$, where K is constant (K= 0.9), λ is the X-ray wavelength of CuKα used in XRD, θ is the Bragg's angle and $\beta$is the full-width at half-maximum (FWHM). The average crystallite size was calculated using Scherer's equation found to be ~23 nm.

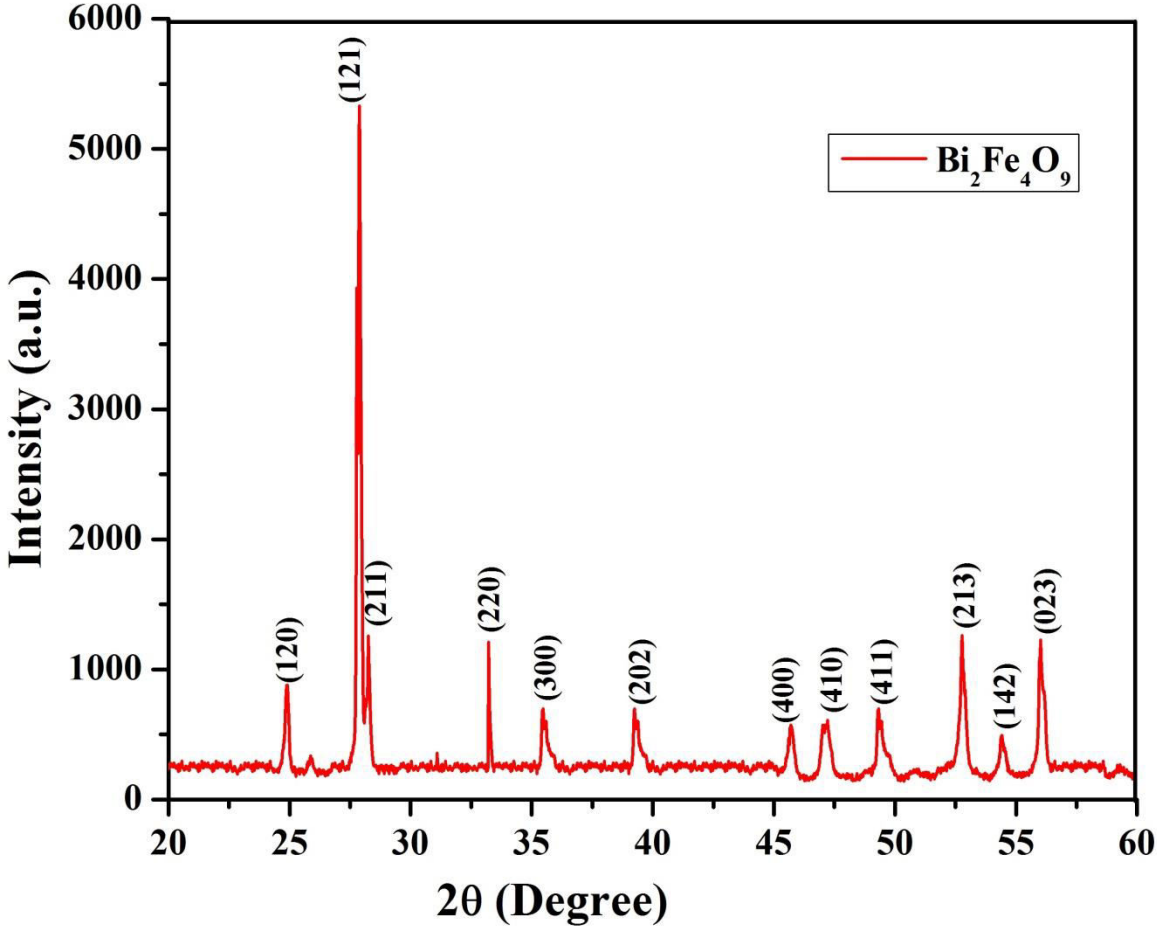

Figure 1 X-ray diffraction patterns of $Bi_2Fe_4O_9$ thin films annealed at 550 ^{0}C.

3.2. Surface topography

3.2.1 Atomic force microscopy (AFM) studies

Atomic force microscopy (AFM) pictures of $Bi_2Fe_4O_9$ thin films produced by spray pyrolysis process are shown in Figure 2(a)-(b). The micrograph indicates that nanorods like growth of $Bi_2Fe_4O_9$ thin films with distinct grain and grain boundary topographies are dispersed across the sample surface. Additionally, as the annealing temperature is raised, the density and growth of nanorods in the film's increase, as seen in figure 2(a-b). The $Bi_2Fe_4O_9$ sample that was annealed at 500°C and 550°C yielded estimated particle sizes of around 200 nm and 300 nm, respectively, based on the AFM image. As a result, the increases in particle size as well as density of the films with increasing annealing temperature. The surface characteristics of $Bi_2Fe_4O_9$ thin films annealed at 500 °C and 550 °C, such as the root mean square (RMS) surface roughness, were computed and determined to be approximately 6.76 nm to 8.67 nm, respectively. This roughness increase with increasing annealing temperature is a sign that the $Bi_2Fe_4O_9$ thin-film surfaces are becoming more defective.

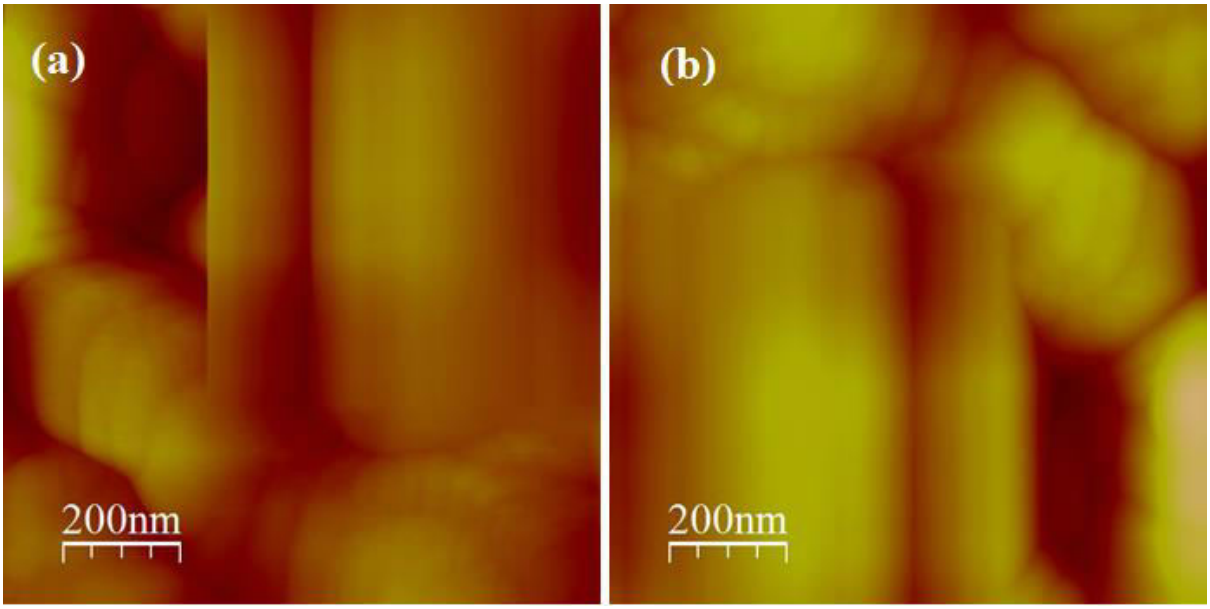

Figure 2(a-b) 2-D AFM surface topography of $Bi_2Fe_4O_9$ thin films annealed at 500^0C and 550 ^{0}C.

The high resolution contour plot of $Bi_2Fe_4O_9$ thin films, shown in Figure 3(a)-(b), shows that the grains in grow symmetrically in plane shapes with elliptical bases. The elliptical bases of the in-plane forms and their symmetric growth are amplified in the $Bi_2Fe_4O_9$ thin film contour plot.

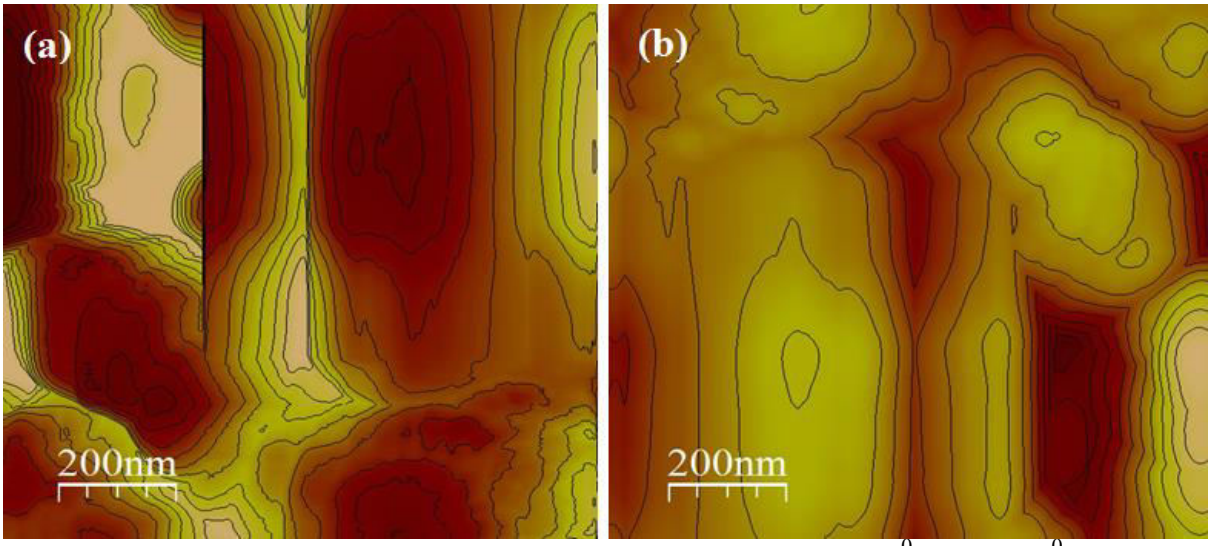

Figure 3(a-b) Contour plot of $Bi_2Fe_4O_9$ thin films annealed at 500 ^{0}C and 550 ^{0}C.

The 3-D AFM pictures shown in Figure 4(a) and 4(b) show that the distribution of $Bi_2Fe_4O_9$ NPs uniform grains of nanorods has an average height of 24.0 nm and 38.8 nm. Grain growth may be the source of the Z-height distribution's alteration and slight increase. As a result, fractal analysis can be used to statistically analyze the grain distribution and provide details on the grain's random distribution.

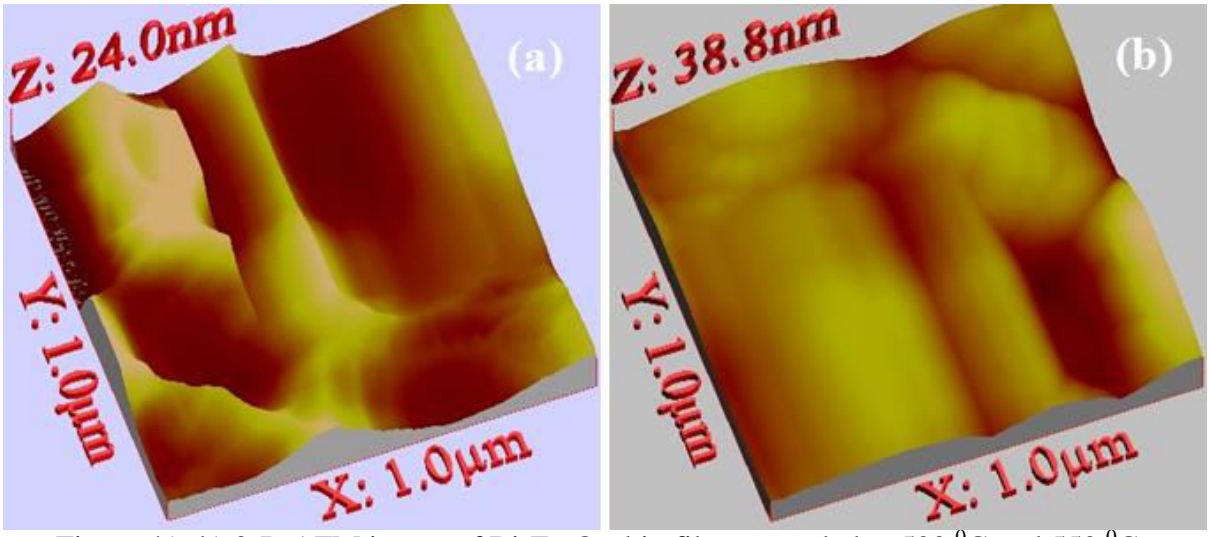

Figure 4(a-b) 3-D AFM image of $Bi_2Fe_4O_9$ thin films annealed at 500 ^{0}C and 550 ^{0}C.

3.2.2 Fractal Analysis

The fractal analyses of $Bi_2Fe_4O_9$materials are shown in Figures 5(a) and 5(b) utilizing the Power Spectral Density (PSD) method and increasing the $Bi_2Fe_4O_9$ sample's annealing temperature from 500 °C to 550 °C. The ability to take into account the intricate fracture morphology of the surfaces is one of the fractal approach's benefits. The spatial distribution of grain inside the thin film, crystal size, and the combined impacts of morphology determine the fractal dimension, which is one possible indicator of the degree of surface roughness. Fractal dimension can be computed using the power spectral density (PSD) approach. A bigger D denotes a more uneven and fragmenting surface [14]. In this method, fractal dimension (D) ranging from 2 to 3 is effective to display the irregularity of the surface morphology.The foundation of the PSD approach is the idea that the infinite frequency mode superimposes a fractal surface morphology. Power spectrum density Sω and its matching frequency ω have a connection that is dependent on D. The values of S_ω and ω have relationship as follows:

$$S_\omega \propto \omega^{-(5-2D)}$$

Where D is fractal dimension of the film, the experimental surface is fractal at defined lengthscales of fractal behavior.Outside of these lengths the surface behaves like a flat surface.

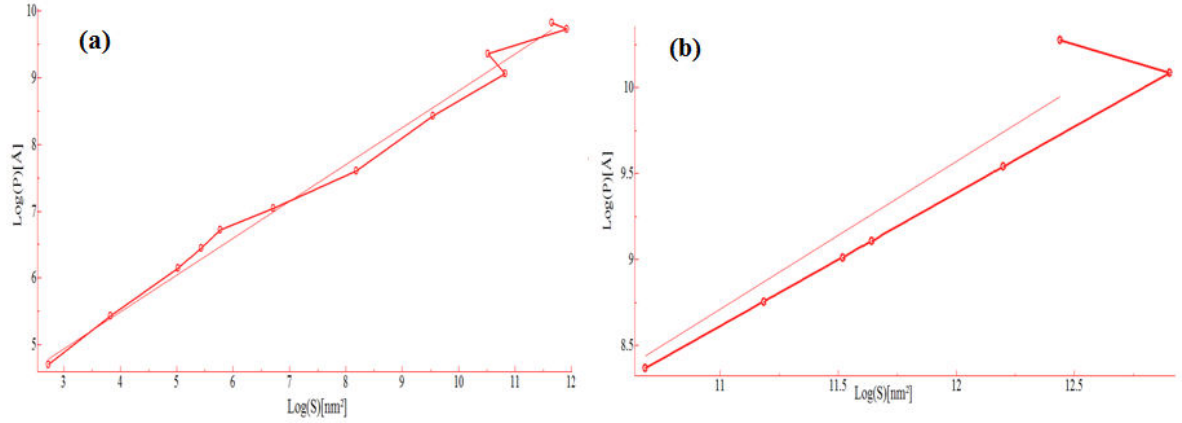

Figure 5 (a-b)Fractal analyses of $Bi_2Fe_4O_9$ thin films annealed at 500 ^{0}C and 550 ^{0}C using Power spectral density (PSD) method.

It is evident from the fractal dimension numbers of 1.78 and 2.06that the fractal dimension is expanded by rising values. This finding suggests that can be used to characterize how the whole grain shape varies along the growth direction. Furthermore, the fractal dimension has spatial and profile deviation information, in contrast to RMS roughness. Thus, the surface abnormalities are usefully described by the fractal analysis. Fractal analysis is more accurate than traditional processing since it calculates the fractal dimension over all scaling ranges, as was previously mentioned.

4. Conclusion

We successfully synthesized $Bi_2Fe_4O_9$ thin films in our present research employing the spray pyrolysis methods. $Bi_2Fe_4O_9$ thin film single phase synthesis with a rhombohedral crystal structure and an R-3m space group is confirmed by XRD. According to Scherer's equation, the average crystallite sizes were determined to be 23 nm. An increase in annealing temperature causes the RMS surface roughness to increase from around 6.76 nm to 8.67 nm, indicating a modification in the thin film's crystal structure. The AFM image revealed the fractal dimension values, which were 1.78 and 2.06. This indicates that when the sample's annealing temperature increases from 500 °C to 550 °C, the fractal dimension increases. This outcome can be used to characterize how the whole grain shape varies along the growth direction. Furthermore, the fractal dimension has spatial and profile deviation information, in contrast to RMS roughness. The multiferroic material may found use in modern devices based as evidenced by the decrease in RMS surface roughness observed in the $Bi_2Fe_4O_9$ sample when the annealing temperature was raised from 500 °C to 550 °C.

Acknowledgements

The authors are highly thankful to Department of Physics,University of Lucknow, Lucknow for providing synthesis and characterization facility, X-RD and AFM measurement.

References

[1] G. Lawes and G. Srinivasan, Introduction to magnetoelectric coupling and multiferroic films, J. Phys. D Appl. Phys. 44 (2011) 243001–243022.

[2] J. Ma, J. Hu, Z. Li, and C.W. Nan, Recent progress in multiferroic magnetoelectric composites:From bulk to thin films, Adv. Mater. 23(9) (2011) 1062–1087.

[3] C.C. Zhou, B.C. Luo, K.X. Jin, X.S. Cao, and C.L. Chen, Magnetic and dielectric properties of $BiFeO_3$–$La_{1/3}Sr_{2/3}MnO_3$ hybrid composite ceramics, Solid StateCommun. 150 (2010) 1334-1337.

[4] A.K. Singh, S.D. Kaushik, B. Kumar, P.K. Mishra, A. Venimadhav, V. Siruguri, and S. Patnaik, Substantial magnetoelectric coupling near room temperature in $Bi_2Fe_4O_9$, App.Phys. Lett. 92 (2008) 132910-132913.

[5] T. Liu, Y. Xu, and C. Zeng, Synthesis of $Bi_2Fe_4O_9$via PVA sol–gel route, Mater. Sci.Eng. B 176 (2011) 535-539.

[6] Z. Yang, Y. Huang, B. Dong, H.L. Li, and S.Q. Shi, Densely packed single-crystal $Bi_2Fe_4O_9$ nanowires fabricated from a template-induced sol–gel route, J. Solid State Chem. 179 (2006) 3324-3329.

[7] Y. Xiong, M.Z. Wu, Z. M. Peng, N. Jiang and Q.W. Chen, Hydrothermal synthesis andcharacterization of $Bi_2Fe_4O_9$ nanoparticles, Chem. Lett. 33 (2004) 502–503.

[8] R.R. Awasthi, B. Das, Structural transition and tunable optical, morphological and magnetic properties of Mn-doped $BiFeO_3$ films, Optik 194 (2019) 162973.

[9] R.R. Awasthi, K. Asokan, B. Das,Structural, dielectric and magnetic domains properties of Mn-doped $BiFeO_3$ materials, International Journal of Applied Ceramic Technology 17 (2020) 1410.

[10] H. Naganuma, J. Miura, and S. Okamura, Ferroelectric, Electrical and Magnetic Properties of Cr, Mn, Co, Ni, Cu Added Polycrystalline $BiFeO_3$ films, Appl. Phys. Lett. 93 (2008) 052901.

[11] R.R. Awasthi, K. Asokan, B. Das, Effect of molar concentration on structural, magnetic domain and optical properties of $BiFeO_3$ thin filmsApplied Physics A 125 (2019) 338.

[12] R.R. Awasthi, B. Das,Effect of temperature on physical properties of $Bi_2Fe_4O_9$ polycrystalline materials, Journal of the Australian Ceramic Society56 (1) (2020) 243.

[13] R.R. Awasthi, S.K. Trivedi, V.S. Chandel, M. Shariq, H.J. Alathlawi, S.P. Singh,Effect of Zn doping on structural/microstructural, surface topography, and dielectric properties of $Bi_2Fe_4O_9$ polycrystalline nanomaterials. ACS omega. 8 (2023)15960-15967.

[14] C.L. Jing, W. Tang, Ga-doped ZnO thin film surface characterization by wavelet and fractal analysis, Appl. Surf. Sci., 364 (2016) 843-849.